Materials Today Communications 33 (2022) 104863

Contents lists available at ScienceDirect

Materials Today Communications

journal homepage: www.elsevier.com/locate/mtcomm

Smart fiber orientation monitoring system in a mold via electrical route modeling

Hyung Doh Roh [a], In Yong Lee [b], Jungwan Lee [a], Jung-soo Kim [a], Young-Bin Park [b,*], Moon-Kwang Um [a,*]

[a] Carbon Composites Department, Composites Research Division, Korea Institute of Materials Science (KIMS), Changwon, Gyeongnam 51508, Republic of Korea
[b] Mechanical Engineering, Ulsan National Institute of Science and Technology (UNIST), Ulsan 44919, Republic of Korea

ARTICLE INFO

Keywords:
Carbon fibres
Electrical properties
Sensing

ABSTRACT

The orientation of unidirectional carbon fibers (UDCFs) in a manufacturing process is critical to the mechanical properties of carbon fiber reinforced plastics (CFRPs). This study presents a method to monitor the orientation of UDCFs on a mold using electrical resistance during the CFRP manufacturing process. An equivalent electrical model for UDCFs was proposed to develop an in situ sensor in a mold. The orientation of UDCFs during the CFRP manufacturing process is investigated in terms of its orthotropic electrical properties. The proposed technique can have strong implications on in situ monitoring of composite molding process where the fiber orientation is unseen by monitoring electrical resistance with Cu tapes as electrodes.

1. Introduction

Carbon fiber reinforced plastics (CFRPs) possess a large strength-to-weight ratio. Therefore, it is being increasing used in fields such as aircraft [1,2], automobile [3], and civil infrastructure [4]. However, continuous carbon fiber as a reinforcing material for CFRPs exhibits superior mechanical properties only in the lengthwise direction. For example, the intermediate-modulus type carbon fiber has a tensile modulus of 200–300 GPa, and a tensile strength of 3–4 GPa [5]. In contrast, the transverse mechanical properties of a CFRP are not as strong [6]. Hence, the design consideration of CFRPs must include the orthogonal mechanical properties.

Composite manufacturing can help realize the advantages of CFRPs in different directions [7–9]. To allay safety and cost concerns, the final product must not deviate from the design [8,10–12]. That is, the process from CFRP design to manufacturing must be monitored. Although studies have explored the monitoring process [13,14], most have focused on resin curing monitoring [15–18] or on the residual stress during resin curing [19,20], However, fiber angle monitoring is the most critical area that needs focus, as the reinforcing material undergoes mechanical loading [21].

A few studies [22–25] investigated the quality of CFRP manufacturing systems using eddy currents or ultrasonic guided waves. Their scanning resolution was as precise as fiber waviness can be identified. Another study measured Young's modulus during curing [25]. However, they did not investigate the real-time fiber alignment monitoring as they focused on the analytic approach with eddy currents after the CFRP manufacturing.

The use of electrical resistance to monitor carbon fiber composites has been investigated [26,27]. For example, Ali *et al.* [26] proposed an electrically equivalent circuit model to predict the permeability of the fabric. The measured resistance was correlated to the porosity of the material, which was a fabric consisting of a composite material. Another study led to the development of a method that enabled the structural health of a material to be monitored by electrical impedance tomography [27]. Specifically, the use of the electrical conductivity, which is the reverse of resistivity, was investigated to localize the impact damage. The principle underlying this study was that the structural change affected the electrical network. However, these studies are *a posteriori* and are not suitable for monitoring a manufacturing process in real time.

Thostenson's group [28–30] also investigated the electrical resistance of carbon fiber composites manufactured by electrophoretic deposition. They developed multiscale hierarchical carbon composites using carbon fibers and carbon nanomaterials. They mainly measured the electrical resistance to monitor the strain and detect cracks [28,29]. In addition, resistance monitoring was utilized to verify the performance of electrodes [30]. Unfortunately, as with the aforementioned studies, Thostenson's group did not use electrical measurements for in-situ

* Corresponding authors.
E-mail addresses: ypark@unist.ac.kr (Y.-B. Park), umk1693@kims.re.kr (M.-K. Um).

https://doi.org/10.1016/j.mtcomm.2022.104863
Received 1 August 2022; Received in revised form 31 October 2022; Accepted 4 November 2022
Available online 8 November 2022

real-time monitoring of composite manufacturing.

This study investigated the alignment of carbon fiber on a mold using electrical resistance. Moreover, an electrically ultimate route was modeled to estimate the electrical resistance of carbon fiber fabrics in terms of orientation. The electrically ultimate route model is a dominant equivalent circuit of substantial network, i.e., carbon fibers connecting the opposite electrodes in a shortest way. The numerical values from the equivalent circuit model and empirical data were analyzed to develop a smart mold that detects fiber orientation. The mold could monitor the fiber angle by simply monitoring the electrical resistance with Cu tapes. The developed in-situ monitoring system of the fiber alignment which is unseen in the mold before the infusion can significantly contribute to the composite manufacturing process because the fiber mis-alignment is directly relevant to the cost, labor, and mechanical properties.

2. Materials and experiment

2.1. Materials

A T300SC-yarn-type 12 K unidirectional carbon fabric (UDCF; Toray, Japan) was purchased from JMC Corp. (Gyeongju, Korea). The fiber areal weight of the UDCF was 299 g/m^2. It was bonded with polyester ribs in the perpendicular direction for handling. A 3 K plain-woven carbon fabric (PWCF) was woven with T300SC yarns (Toray, Japan) at JMC Corp. (Gyeongju, Korea). A 3 K single carbon fiber tow was isolated from the PWCF. Electrodes for the 4-probe measurement were installed as shown in Fig. 1(a). Carbon-glass hybrid fabric (CGHF) holds carbon fiber tows in either warp or weft form, and glass fiber tows in the other as shown in Fig. 1(b). The CGHF supplied by JMC Corp. (Gyeongju, Korea) was woven with Toray yarns.

2.2. Characterization

Electrical resistance along the tow, expressed as an intratow network, was measured by the 4-probe method (Fig. 1(a)). The electrical resistance per interply network—the resistance divided by the number of stacked fabrics—were also measured (Fig. 1(c)). The electrodes installed in the 4-probe measuring system were Ag paste and Cu wires (Fig. 1(c)). The electrical resistance of the intertow connection between two respective single tows was measured similarly (Fig. 1(d)). The electrical resistance per unit length or the number of plies were measured five times, and the maximum and minimum values were eliminated. The resistance values in terms of the geometry or the number of unit materials were the averages of the values of the three specimens.

For the investigation of a smart mold system, four Cu tapes as electrodes were attached on an electrically insulative glass mold in parallel (Fig. 1(e)). The electrically conductive fabric sets were laid on the Cu tape. Direct-current electrical resistances of the fabrics were measured by the 4-probe system via a multimeter (Keithley 2002, USA), which represents 6.5 significant digit numbers. The fabrics were rotated every 5° clockwise to investigate the electrical resistance. Zero degree is the case when the carbon fiber tows were aligned parallel to the Cu tapes.

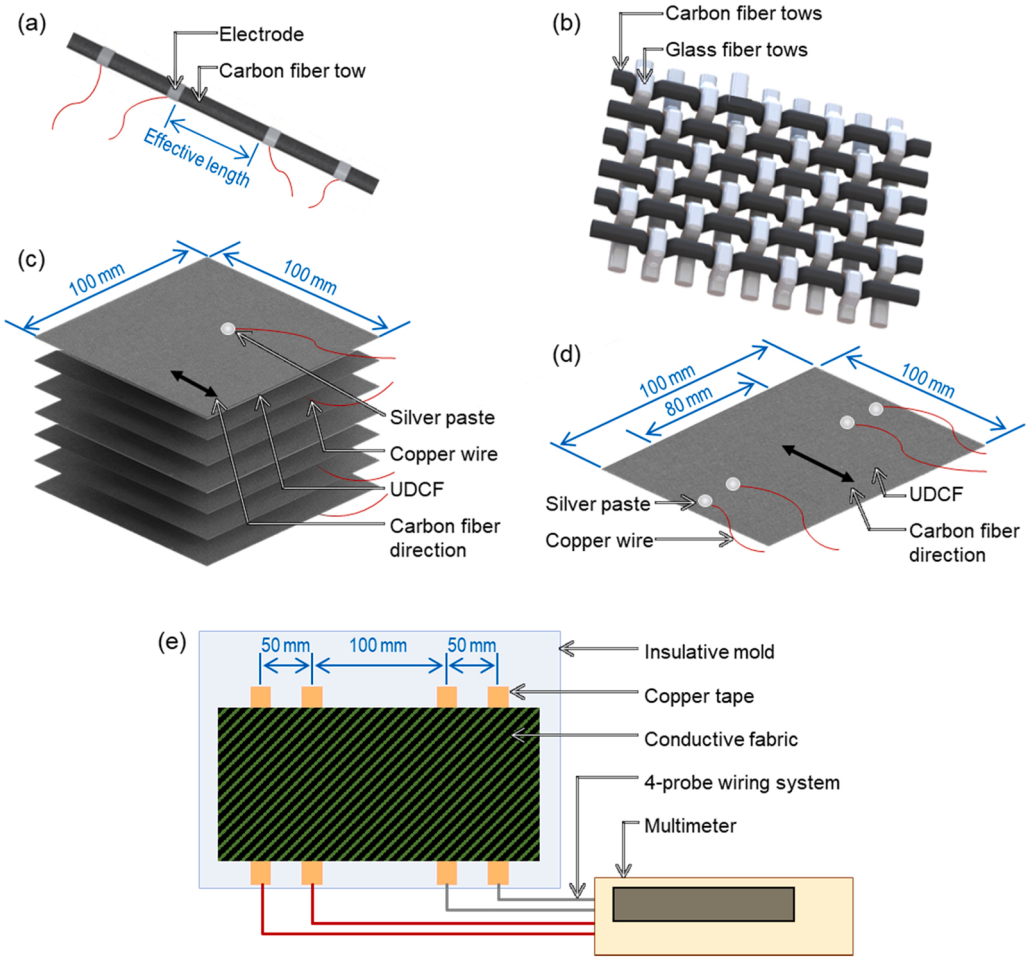

Fig. 1. (a) Single carbon fiber tow, (b) Carbon–glass hybrid fabric and experimental setup for the electrical resistance measurement (c) in the through-thickness direction, (d) in the in-plane intertow direction, and (e) on the mold.

2.3. Hypotheses

Electrical current flows in a carbon fiber of a carbon fabric when voltage is applied to it because the carbon fiber tows in the fabric are electrically conductive. The potential network in the fabric can be along the carbon fiber tow, which is called the intratow network, and connecting the tow, which is called the intertow network.

Two hypotheses were proposed to investigate the electrically ultimate path. The ultimate purpose of the introduction of two different hypotheses was to find the most acceptable electrical network and modeling of the composite by comparing two different hypotheses.

The first one states that the ultimate path is determined by selecting the easiest sole route, indicated by the red line in Fig. 2(a). The least electrical resistance value should be observed with this hypothesis. Hence, the ultimate intratow network should be the longest. Further, the intertow network should have the smallest length.

The other one states that the electrical path lies in all the electrical path, which is in contact with electrodes as shown in the blue lines in Fig. 2(b). The electrical networks start and end where the carbon fibers lie on the electrodes with a combination of numerous intratow and intertow networks.

3. Results and discussion

3.1. Electrical resistor modeling

Electrical networks are forms of carbon fibers modeled into electrical resistors. The carbon fiber single tow shown in Fig. 1(a) represents an average resistance of 1.103 ohm with a standard deviation of 0.054. The effective length of the tow is 110 mm. The resistance per unit length of the single tow, ρ_{tow}, can be measured as 0.01 ohm/mm. Similarly, the resistance per interply network, R_{zint}, measured from Fig. 1(c) is 9.75 ohm/ply. The investigation revealed a resistance of 39 ohm when four UDCFs were stacked together. In metric units, the resistance was 25.66 ohm/mm in the through-thickness direction. The geometry in terms of the length and width of the through-thickness measurement was not considered because the most effective path was localized where the silver paste electrodes were aligned. A resistance of 8900 ohm was observed between 81 parallel tows which shows that the intertow resistance between the adjacent tows, ρ_{inter}, is 111.25 ohm/tow. The distance across which the interply resistance was measured was 80 mm, and hence, ρ_{inter} was 111.25 ohm/mm when the width, which was the length of the Cu electrodes, was 100 mm. The resistance values for the equivalent circuit modeling are summarized in Table 1.

3.2. Electrodes setup: 4-probe and 2-probe method

Electrical resistances of the UDCFs and PWCFs were measured by 4-probe and 2-probe methods to analyze the contact resistance between the electrodes and the carbon fiber fabrics. While the 4-probe method is unaffected by the contact resistance, the 2-probe method measures not only the sample resistance but also the contact resistance. Hence, the aim of this analysis is to investigate the effects of contact resistance.

Table 1
Electrical resistance values for electrically equivalent circuit modeling of carbon fabrics.

ρ_{tow} (Ohm/mm)	ρ_{inter} (Ohm/tow)	R_{zint} (Ohm/ply)
0.01	111.25	9.75

Both the 2-probe and 4-probe methods revealed similar electrical resistances of UDCFs as shown in Fig. 3, despite the 2-probe method measuring higher resistances compared to the 4-probe method.

However, the resistances of PWCFs represented larger discrepancies in the 4-probe and 2-probe methods as shown in Fig. 4. For example, the resistance of the two plies of PWCFs showed a maximum value which is 500 times larger in the 2-probe method compared to the value in the 4-probe method. Thus, the 2-probe method in this study is not suitable to measure the resistances of PWCFs. The 4-probe method was hence adopted in this research.

3.3. Hypothesis analysis and electrical route modeling

Two different hypotheses were proposed and verified to determine the electrical networks in the carbon fiber fabrics. Hypothesis #1 proposes that an electrical route follows the easiest single path. The numerical electrical resistance values were obtained by considering the geometry of the UDCFs and constituting the electrically equivalent circuit model. This model includes the intratow, intertow, and interply electrical networks. Hypothesis #1 suggests that the ultimate electrical network in carbon fabrics is the easiest and sole path along the tows as shown in Fig. 2(a). The verification of hypothesis #1 shown in Fig. 5(a) proves the reasonability of the proposed hypothesis.

Hypothesis #2 proposes that all the carbon fiber tows are involved in the electrical network as electrical resistors connected in parallel. Similar to the model that forms the basis of Hypothesis #1, the equivalent model of Hypothesis #2 includes all the intratow, intertow, and interply factors in terms of the fabric geometry. However, Hypothesis #2 has shown unacceptable discrepancies as shown in Fig. 5(b). These discrepancies are attributed to the enormous number of electrically closed-loop circuits that exist in the fabric, and the fact that Kirchhoff's superposition theorem applies to the loops.

Although Kirchhoff's superposition theorem should have been applied to the model as previously studied at the atomic scale [31,32] which has electrically closed loops, the model on which Hypothesis #2 is based is a summation of the resistance values of combinations of resistors in series and parallel as follows:

$$\frac{1}{R_{total}} = \frac{1}{R_{region1}} + \frac{1}{R_{region2}} + \frac{1}{R_{region3}} + \quad \cdots + \quad \frac{1}{R_{regioni}} \tag{1}$$

where the subscripts "region 1″ to "region i," where i is an integer, represent the summation of the resistance of a local area for which the electrical resistors are arranged in series.

This summation simply adds intertow and intratow networks as

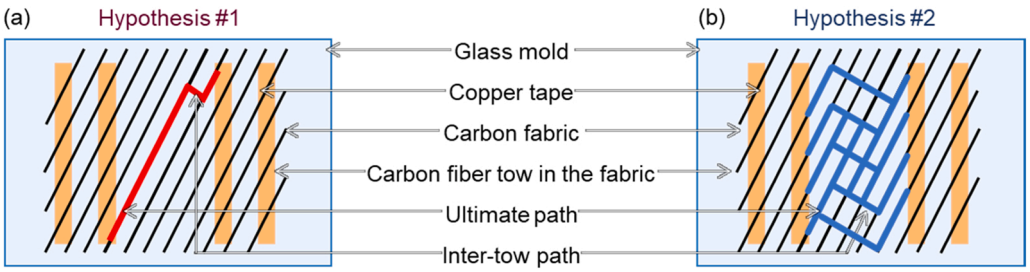

Fig. 2. Hypotheses for the electrical network: (a) the electrical network is determined by the easiest single path, and (b) all the electrically conductive network touching the electrode participate in the electrical network.

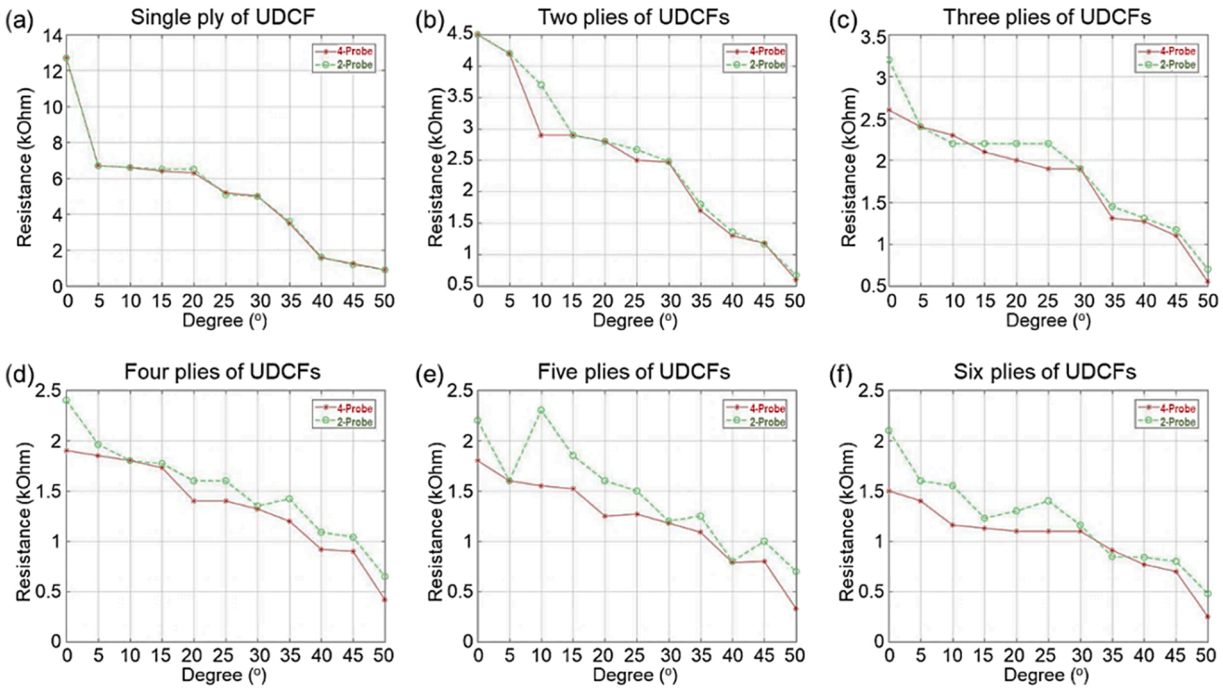

Fig. 3. Electrical resistances of the unidirectional carbon fibers (UDCFs) measured by 4-probe and 2-probe methods in terms of the angle between the tow and the electrodes: (a) single ply, (b) two plies, (c) three plies, (d) four plies, (e) five plies, and (f) six plies.

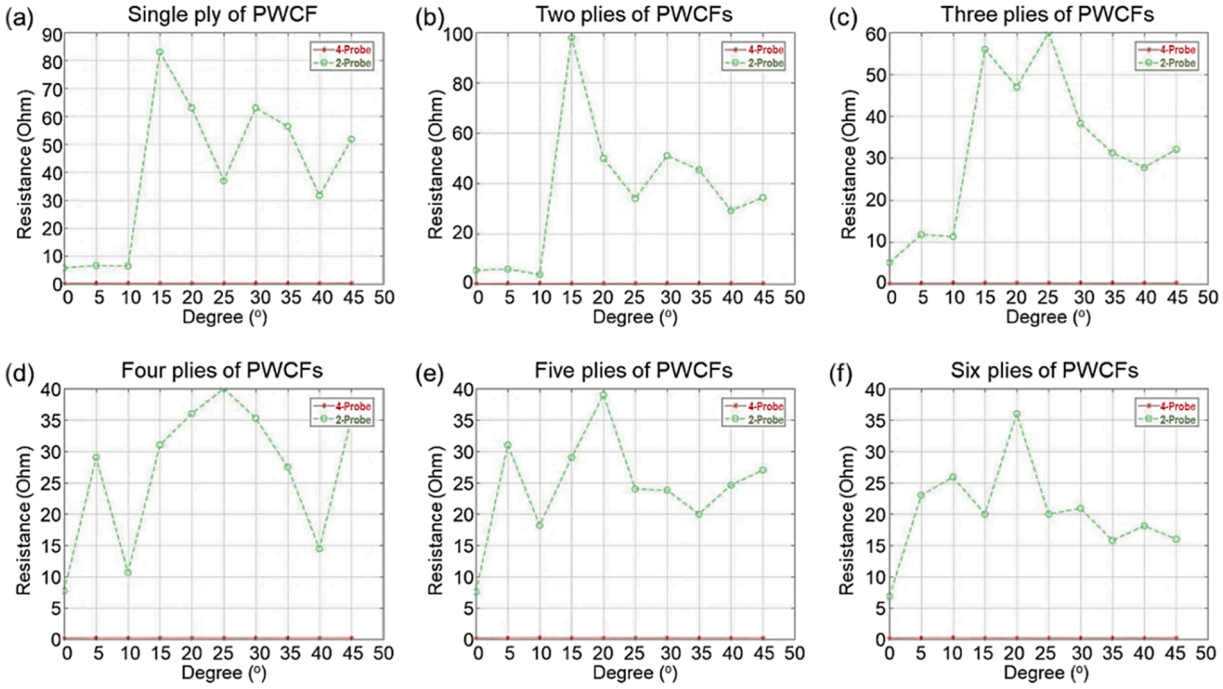

Fig. 4. Electrical resistances of plain-woven carbon fabrics (PWCFs) measured by 4-probe and 2-probe methods in terms of the angle between the tow and the electrodes: (a) single ply, (b) two plies, (c) three plies, (d) four plies, (e) five plies, and (f) six plies.

other research groups proposed [33,34]. In specific, electrical resistivity was multiplied by the geometry of a sample, and different types of electrical networks such as intratow and intertow networks were connected either in series or in parallel. However, this hypothesis double imposes the electrical network because the current flow could be changed with respect to not only Ohm's law and Kirchhoff's current law. In accordance to Ohm's law, the more electrical current might flow in the path with the smaller electrical resistance. Kirchhoff's superposition theorem could identify the current flow in the enormous electrical loops in the fabric. Taking all the electrical parameters underlied in the fabric into account, the maximum electrical current might be observed in the easiest path, which is the single tow path as shown in Hypothesis #1, because Kirchhoff's superposition theorem might indicate that the current at the fabric periphery might be as small as be ignored compared to the electrically easiest path.

Therefore, the result of not applying Kirchhoff's superposition

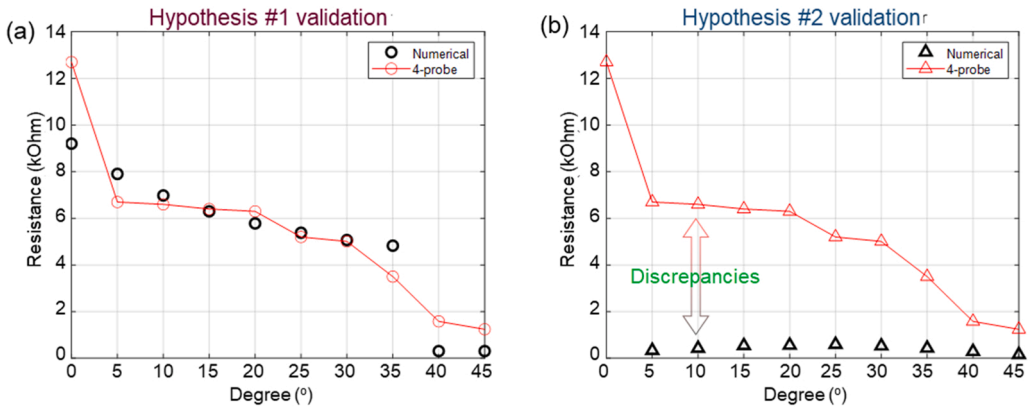

Fig. 5. Validation of the proposed electrical route modeling with UDCFs: (a) Electrical route is determined by the easiest sole path, and (b) Electrical route laid in all the carbon fiber tows contacting the electrodes.

theorem is that an overly large number of electrical networks are imposed in the model of Hypothesis #2, and it led to significant negative errors as shown in Fig. 5(b). Thus, modeling the electrically equivalent circuit should obey the principle of Hypothesis #1 when it is expanded in terms of the metric geometry as proved in the comparative analysis of Hypothesis #1 and #2.

When a single tow connects the inner electrodes on the mold following Hypothesis #1, as shown in Fig. 6(a), the resistance might be written as below:

$$R = \rho_{tow} \times x \tag{2}$$

where R represents the electrical resistance, ρ_{tow} is the electrical resistance of the single tow per unit length, x is the path length, w is the length of the Cu electrode, and s is the span between the electrodes. The angle between the tow and the electrode is represented as ϑ, and the criteria that facilitates the single tow to reaches the opposite electrodes is ϑc. Thus, the path length in the case of Fig. 6(a) can be described as below:

$$s = a \times \sin(\vartheta c) \tag{3}$$

where a is the path along the single carbon fiber tow.

However, when the single tow cannot reach the opposite side such that ϑ is less than ϑc, the intertow network occurs inevitably, as shown in Fig. 6(b). Hence, the resistance might be significantly higher than the case of Fig. 6(a), because of the intertow networks with a resistivity higher than that of the intratow network.

In the case of $[0/90]_N$ crossply, where N is any integer, the perpendicular paths are involved for the minimized electrical resistance, as depicted in Fig. 7(a). The corresponding electrical resistance might be written as below:

$$R = \rho_{tow} \times a_1 + 2R_{zint} + \rho_{tow} \times a_2 \tag{4}$$

where a_1 indicates the path length in the first (bottom) ply, and a_2 indicates the path length in the second ply. In terms of the given geometry, an additional constraint, i.e., span (distance between electrodes), is written as below:

$$s = a_1 \times \sin(\vartheta) + a_2 \times \cos(\vartheta) \tag{5}$$

Then, the resistance can be expressed as below:

$$R = \frac{\rho_{tow}}{\cos(\vartheta)} \times \{a_1 \times (\cos(\vartheta) - \sin(\vartheta)) + s\} + 2R_{zint} \tag{6}$$

In the case of $[0/\varnothing/2\varnothing]_N$ crossply, as depicted in Fig. 7(b), an additional option in the third ply is given. However, if the tow in the second ply reaches the opposite electrode, the tow in the third ply is irrelevant, because the lower electrical resistance contains the less number of interply networks, R_{zint}. Moreover, the symmetric stacking conditions are also applicable despite the irrelevance of the upper parts to the proposed investigation in the same rationale. The effective electrical resistance can be expressed as below:

$$R = \rho_{tow} \times a_1 + 2R_{zint} + \rho_{tow} \times a_2 \tag{7}$$

whose format is equal to that in the case of Fig. 7(a). Due to geometrical constraints, the span can be expressed as below:

$$s = a_1 \times \sin(\vartheta) + a_2 \times \sin(\vartheta + \varnothing) \tag{8}$$

In addition, the constraints in terms of width can be as below:

$$w \geq a_1 \times \cos(\vartheta) + a_2 \times \cos(\vartheta + \varnothing) \tag{9}$$

Furthermore, when more plies are involved in the ultimate path, the

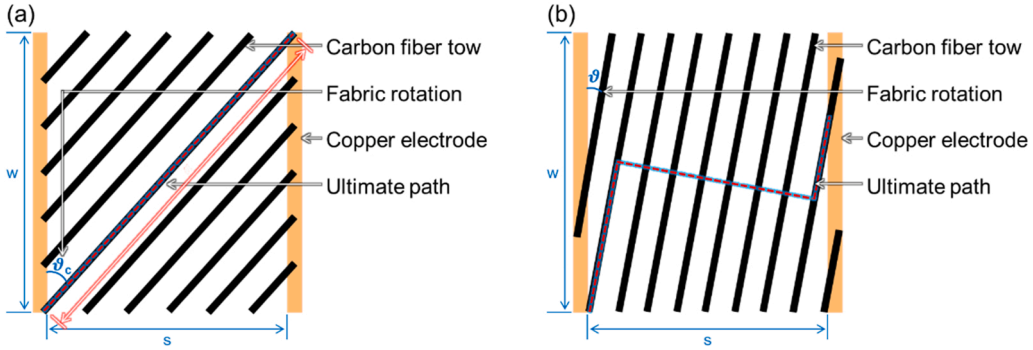

Fig. 6. UDCFs laid on the mold with the following geometrical constraints: (a) the single carbon fiber tow reaches two opposite electrodes, and (b) the intertow network in inevitable.

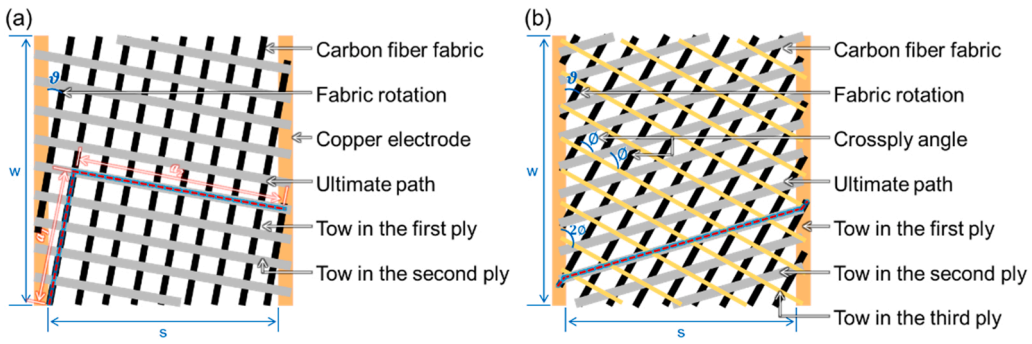

Fig. 7. Fabrics laid on the mold: (a) $[0/90]_N$ crossply, and (b) $[0/\varnothing/2\varnothing]_N$ crossply.

resistance can be as below:

$$R = \rho_{tow} \times \sum a_n + 2R_{zint} \times (n-1) \tag{10}$$

where n is an integer of which the number of plies are related, and a_n is the ultimate path length in the nth ply. The constraints in terms of the geometry are as below:

$$s = \sum a_n \times \sin\{\vartheta + (n-1) \times \varnothing\} \tag{11}$$

3.4. Two-dimensional orientation analysis

3.4.1. Orientation of UDCFs

The electrical resistances of the UDCFs measured by the 4-probe method in terms of fiber orientation are displayed in Fig. 8. Additionally, the numerical calculations based on Hypothesis #1, introduced in Fig. 2(a), were investigated in terms of both fiber orientation and the number of stacked fabrics (Fig. 8).

As the fabric orientation increased, the number of intertow networks reduced under the given geometrical constraints shown in Fig. 6(a) compared to (b). Consequently, the electrical resistance decreased as the angle between the fiber and the electrodes increased. Furthermore, when the single tow bridged the opposite electrodes as depicted in Fig. 6 (a), the electrical resistance abruptly decreases at 40°, 45°, and 50° in Fig. 8. This is because the electrical resistance per unit length as to intertow network was eradicated in the electrically equivalent model by facilitating the single tow to reach the opposite electrode directly.

When the number of stacked plies increased from a single ply to six, as illustrated in Fig. 8(a) to (f), the empirical and numerical electrical resistances decreased. The possibility of contacting the adjacent carbon fiber tows in both in-plane and interply networks increased. In other words, the more the stacked plies, the more the options for the easiest route. Furthermore, the more number of stacked fabrics that weighed more than the single ply, the more stable resistances could be measured.

3.4.2. Orientation of CGHFs

The measured electrical resistances of the CGHFs were as similar to those of the UDCFs, as only carbon fiber tows in the direction of warp or weft were involved in the electrical network, which posses a form similar to that of the UDCF. However, the result of the single ply of the CGHF exhibited theoretically infinite resistance at 0–35°, which implies the absence of an electrical network. The carbon fiber tows in the CGHFs were perfectly separated without any intertow network as the glass fiber tows aided the fiber alignment. This empirical value was also reflected in the equivalent circuit modeling, as illustrated in Fig. 9(a). Moreover, in

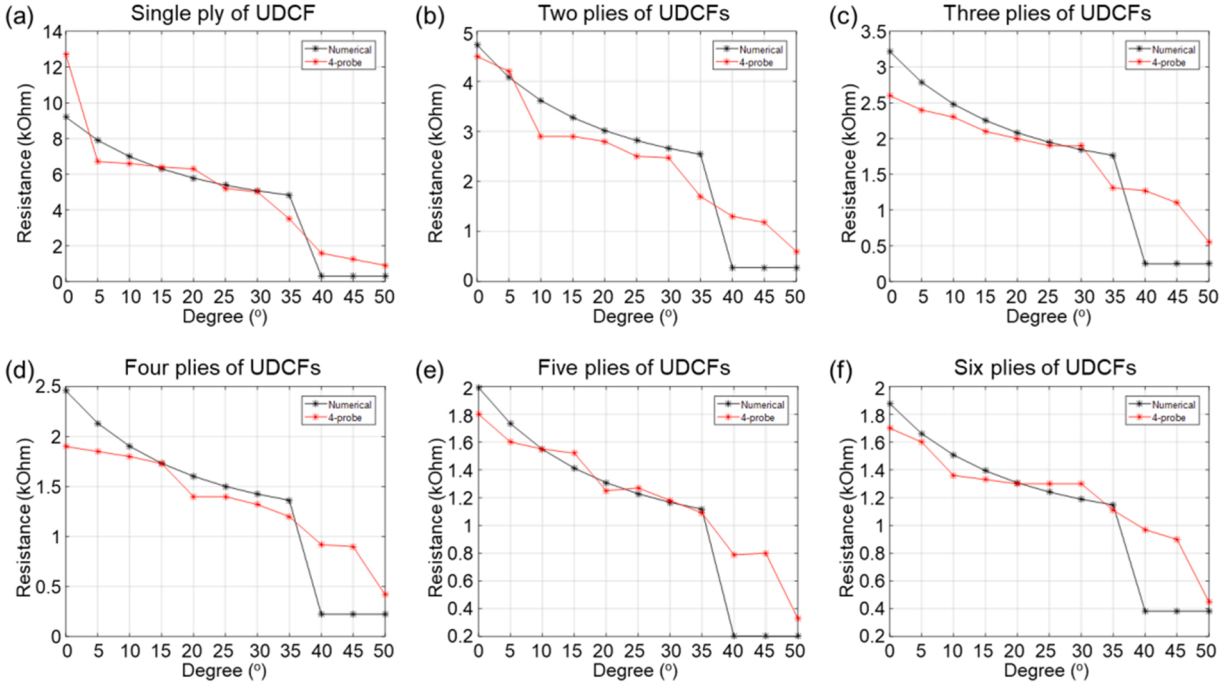

Fig. 8. Electrical resistances of UDCFs numerically calculated using Hypothesis #1 and measured by 4-probe in terms of the angle between the tow and the electrodes: (a) single ply, (b) two plies, (c) three plies, (d) four plies, (e) five plies, and (f) six plies.

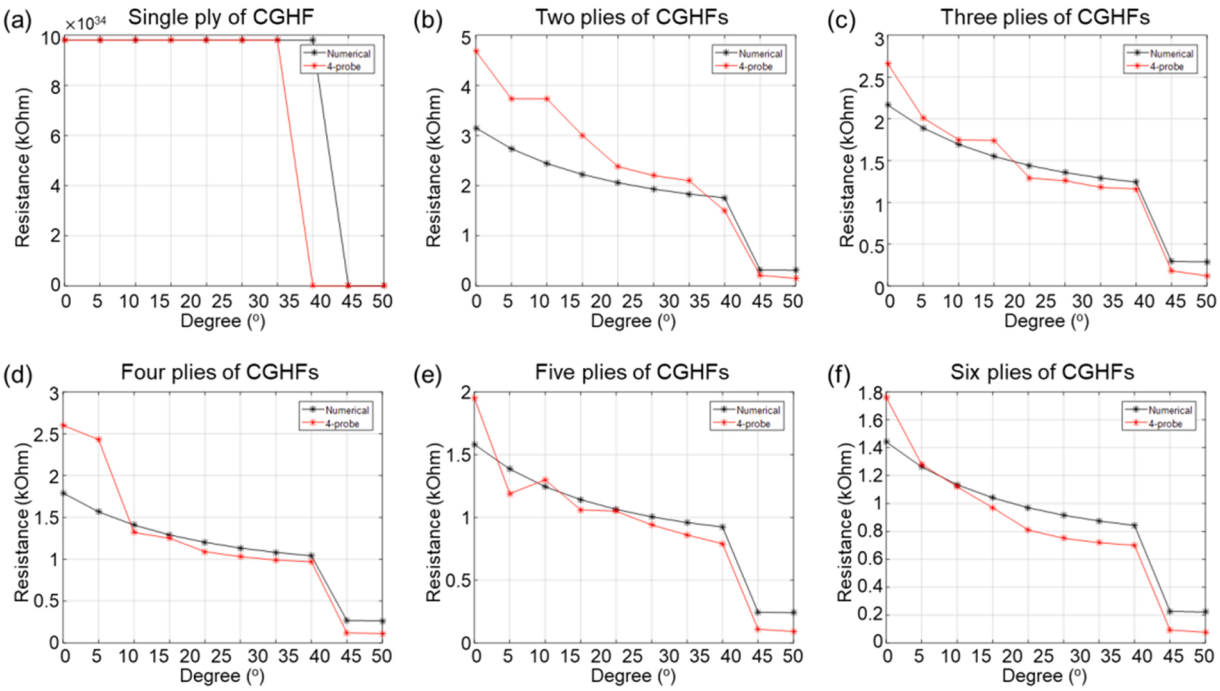

Fig. 9. Electrical resistances of CGHFs numerically calculated using Hypothesis #1 and measured by 4-probe in terms of the angle between the tow and the electrodes: (a) single ply, (b) two plies, (c) three plies, (d) four plies, (e) five plies, and (f) six plies.

the measured and calculated resistances of CGHFs, the authors observed that the resistance decreased by an angle of approximately 45° because of the elimination of the intertow network. The resistances in accordance with the number of stacked fabrics exhibited a behavior similar to that of the UDCFs (Fig. 9).

3.4.3. *Orientation of PWCFs*

The electrically equivalent circuit model of the PWCF exhibited constant electrical resistance values, represented by the black plots in Fig. 10. In other words, the carbon fiber tows in the PWCF secured a stable electrical network between the electrodes. However, the PWCFs produced larger errors between the estimated and measured values, as represnted by the red plots in Fig. 10. For example, an error of approximately 50% was observed (Fig. 10(b)) when the two plies of PWCF aligned parallel to the electrodes. However, the errors decreased as the number of stacked fabrics increased, while a maximum error of

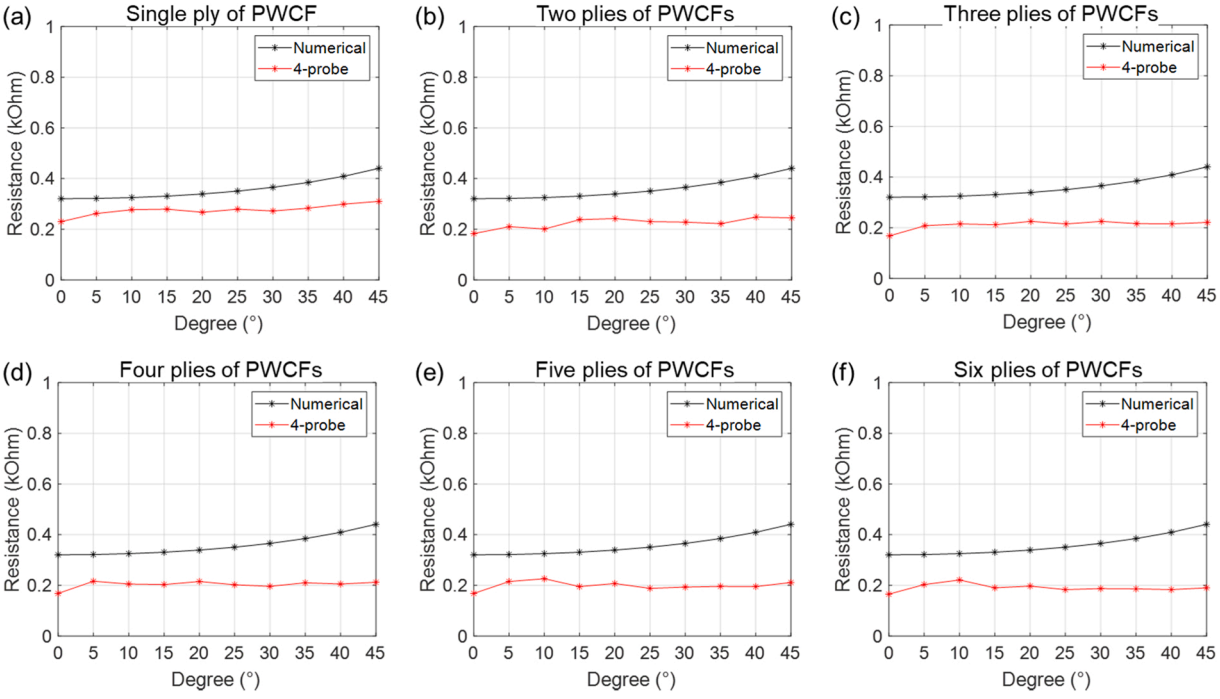

Fig. 10. Electrical resistances of PWCFs numerically calculated using Hypothesis #1 and measured by 4-probe in terms of the angle between the tow and the electrodes: (a) single ply, (b) two plies, (c) three plies, (d) four plies, (e) five plies, and (f) six plies.

22% was observed in Fig. 10(f).

The equivalent circuit model of the PWCF has identical electrical networks along the weft and warp. However, the PWCF has better electrical conductivities than expected, as displayed in Fig. 10. The PWCF was perpendicularly woven, which secured the electrical conductivity in various directions.

The developed model was investigated by converting the empirical intertow resistance per unit length to the intratow data. This sweeping analysis determines the applicability of the developed model to various fabrics such as the UDCF and PWCF, which possess different directional electrical characteristics.

Fig. 11(a) illustrates the sweeping results of Hypothesis #1. This analysis converted the intertow resistance per single tow of the UDCF to the intratow resistance per unit length equivalent, which converges to the resistance values of the PWCF. The smaller black circles in Fig. 11(a) represent the data of sweeping the electrical information between UDCF and PWCF. The circle on the top of each angle represents the estimated resistances of the UDCFs. The circle at the bottom of each angle indicates the estimated resistances of the PWCFs. In other words, the larger blue circles and the blue diamonds denote the estimated resistance values of the UDCF and the PWCF, respectively. Hence, the developed electrical model, Hypothesis #1, successfully estimates the electrical resistance of different fabrics at various orientations.

Fig. 11(b) displays the results of the sweeping analysis based on Hypothesis #2. The finer details of the results are illustrated in Fig. 11(c). The triangles at the top and bottom reveal the electrical information of the UDCF and PWCF, respectively. As in Fig. 11(a), the sweeping results between the UDCF and the PWCF are marked by triangles (Fig. 11(b) and (c)). Although the estimated resistances of the PWCF were similar to the empirical data, the numerical calculation of the UDCF revealed unacceptable discrepancies, as depicted in Fig. 11(b).

In addition, the resistance curve against the fabric angle might vary with the electrical resistivities of the intertow and intratow networks, as illustrated in Fig. 11(d). When the intertow resistance per single tow increases with the fabric used, the overall electrical resistance increases, depicted by black x marks in Fig. 11(d). However, the change in the intratow resistance per unit length might be insignificant as the five pink triangles overlap on the same position, as represented in Fig. 11(d).

3.5. Three-dimensional route analysis with crossplies

The numerical modeling of the crossplies with the stacking configuration of [0/45/90/− 45] were investigated (mesh plots in Fig. 12). The numerical resistance values were analyzed when the crossply stacks were rotated by M° from the electrodes. Table 2 lists the numerically calculated minimum resistance values and the route in the first and second plies. This analysis underlies the proposed model.

The minimum resistance values in Fig. 12 or Table 2 are similar to the empirical results of the four plies of the UDCFs in Fig. 8(d). The empirical data for various stacking angles are also marked with yellow dots in Fig. 12. Therefore, the case of M = 0° in Fig. 10(a) should be similar to the case of M = 45° in Fig. 8(d). The only difference is the addition of the interply network to Fig. 8(d) because the electrically ultimate path is determined to be the easiest path.

The results in Figs. 11 and 12 represent the extensibility of the proposed smart mold to various conditions. The applicability of the proposed mold to different types of fibers was verified by varying the directional electrical resistivity as shown in Fig. 11(a). The applicability of the proposed mold to other fiber stacking angles was proven by changing the angle of fabric sets as shown in Fig. 12. Moreover, the proposed analysis could be extended to different numbers of fiber plies. Three-dimensional electrical routes exist near the surface where the Cu electrodes are located because, as mentioned before in Hypothesis #1, the ultimate path underlies the easiest route. Hence, the ultimate electrical path might underlie the first and third plies near the electrodes as proven by the results in Fig. 12 and Table 2. Therefore, the proposed

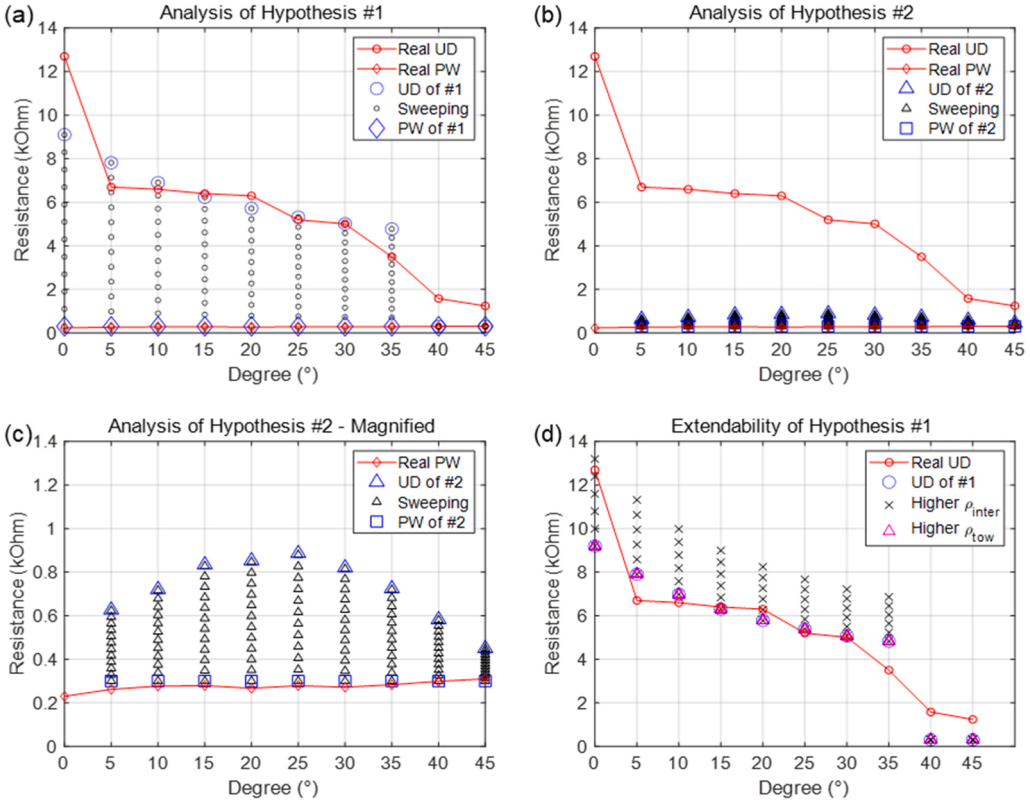

Fig. 11. Sweeping results of the analyzed models with varying intertow resistivity: (a) Analysis of Hypothesis #1, (b) #2, and (c) magnified view of (b). (d) Sweeping analysis of Hypothesis #1 by varying the resistance per single tow and per unit length of the intertow and intratow networks, respectively.

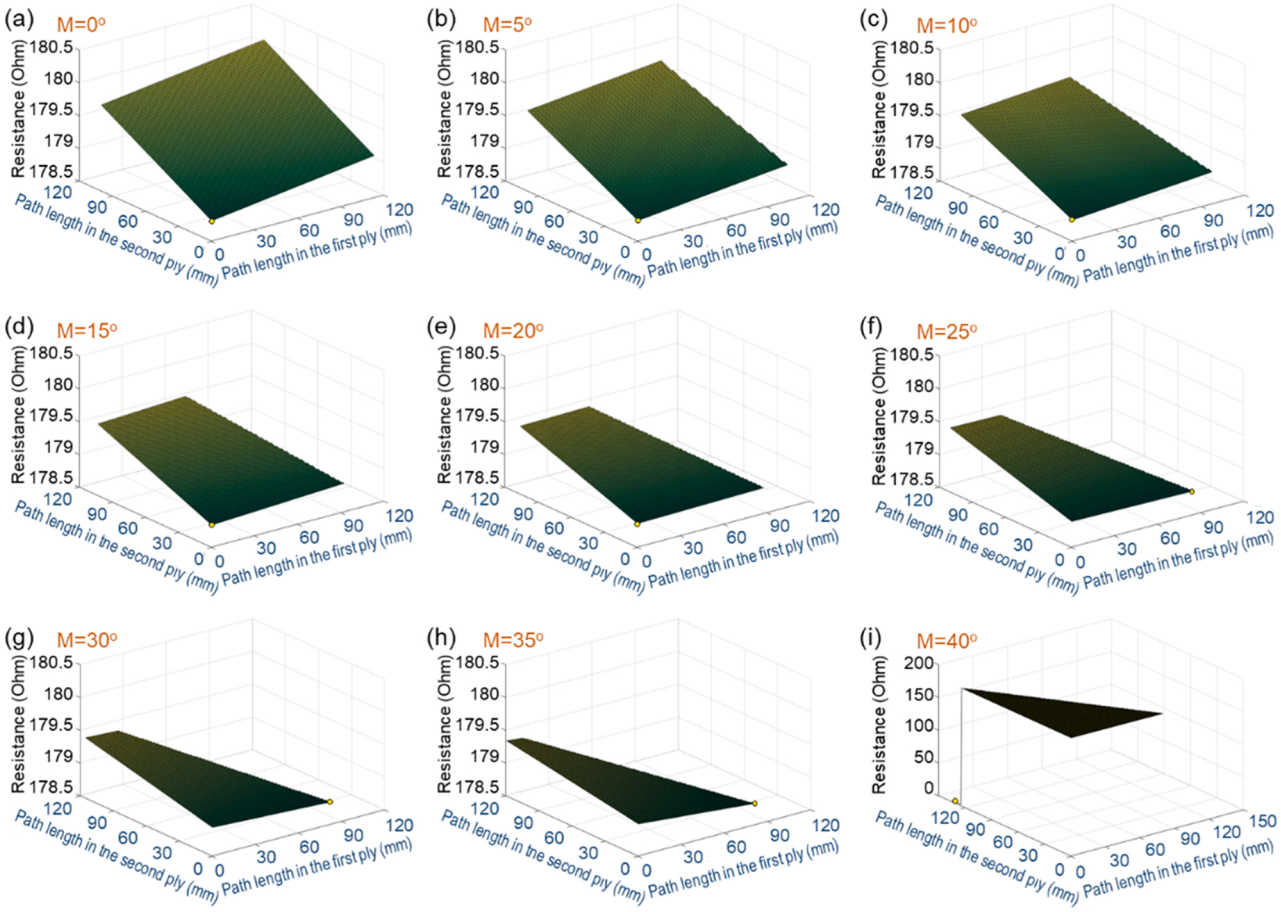

Fig. 12. Electrical resistances of [0/45/90/− 45] crossplies numerically calculated from Hypothesis #1 (mesh) and measured by 4-probe when the fabrics stacked are misoriented by M° (indicated by the yellow dot).

Table 2
Numerical electrical resistance calculated from the electrical equivalent model of [0/45/90/− 45] crossplies.

Orientation (°)	0	5	10	15	20	25	30	35	40
Electrical resistance (Ohm)	178.8	178.8	178.8	178.8	178.9	178.9	178.8	178.8	1.25
Path length in the 1st ply (mm)	0	0	0	0	0	85	82	81	0
Path length in the 2nd ply (mm)	0	0	0	0	0	0	0	0	125

method is expected to be widely applicable to the manufacturing processes of various types of carbon fiber composite materials. The acceptable variables are the number of plies that are stacked, type of electrically conductive fabric, fabric stacking sequence, angle of the fabric sets, and molding system, such as a vacuum film or closed mold, on the top fabric.

4. Conclusions

The electrical resistances of UDCFs, CGHFs, and PWCFs were investigated in various directions, and consequently a smart mold system for CFRPs was proposed. In other words, an equivalent circuit model with electrical route modeling was proposed for dry carbon fabrics. The electrically ultimate route was determined to be the easiest path which means the lowest electrical resistance, and hence the proposed modeling considered only the most electrically conductive route. The electrical resistances of crossplies were numerically obtained, and thus the model was verified.

This study is applicable as an in situ fabric orientation monitoring system in a mold that cannot use visual inspection. Applications include close- and open-mold systems where stacked fibers cannot be observed. The authors estimated the orientation based on the proposed model in Fig. 13 by analyzing the electrical resistance of the fabric with the given electrical information.

The strong point of the proposed technique can minimize the cost, labor, and the risk of fiber mis-alignment by simply measuring electrical resistance. However, this method is not applicable to electrically isotropic materials such as sheet molding compounds or short fiber mats because they represents identical electrical resistance even though they are rotated. Monitoring the angle of electrically isotropic materials can be a candidate of future studies.

In another future study, electrical resistance should be studied in terms of the process of resin infusion to complete the entire CFRP manufacturing process in a mold. The electrical resistance varies in terms of the angle and resin viscosity. Additionally, impregnation of resins into fibers will alter the electrical network. Therefore, developing a smart mold for CFRP curing and fiber orientation is a viable research direction.

CRediT authorship contribution statement

Hyung Doh Roh: Sample manufacturing, mechanical testing,

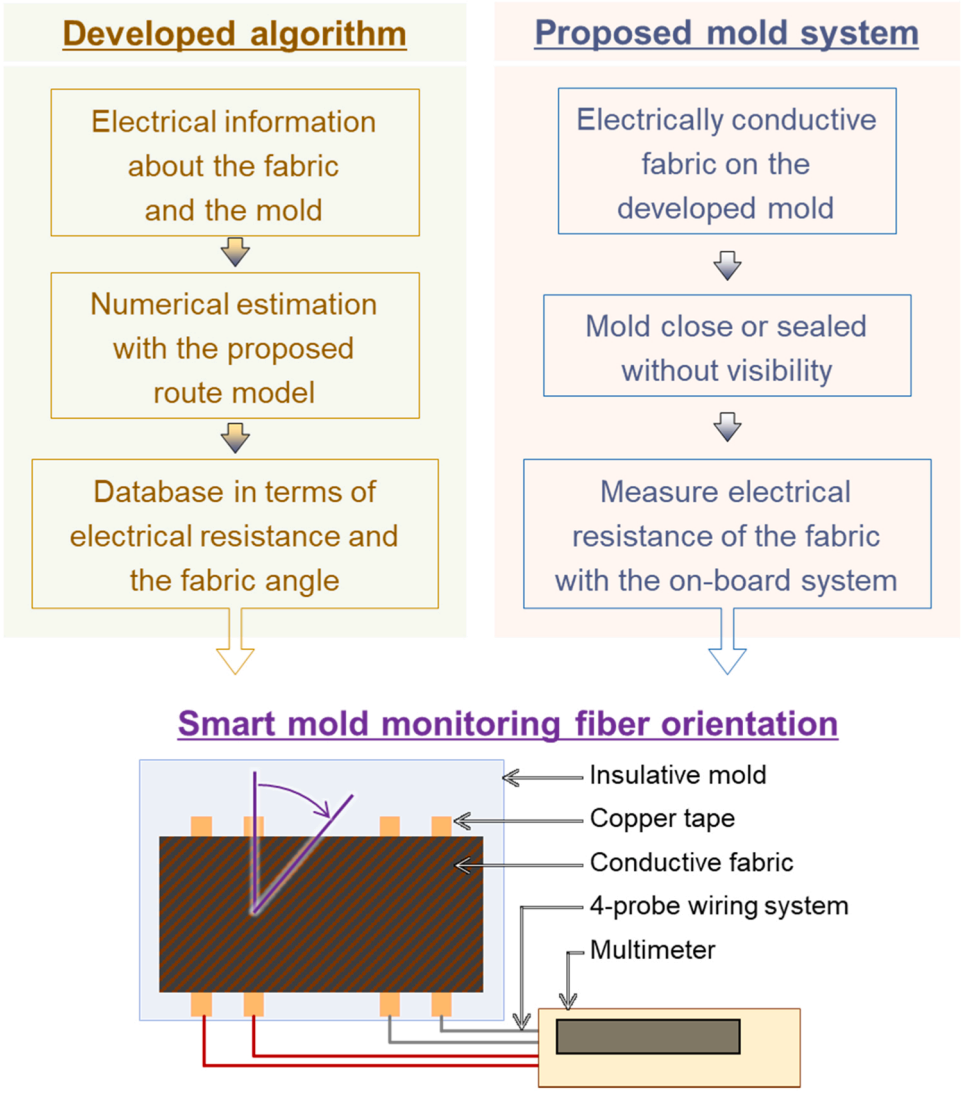

Fig. 13. Working principle of the proposed smart mold.

electromechanical analysis, writing, reviewing, and editing. **In Yong Lee**: Sample manufacturing and electrical resistance monitoring. **Jungwan Lee**: Mechanical testing and editing. **Jung-soo Kim**: Sample manufacturing and electrical resistance monitoring. **Young-Bin Park**: Supervision as a corresponding author. **Moon-Kwang Um**: Supervision as a corresponding author. All authors read and approved the final manuscript.

Declaration of Competing Interest

The authors declare that they have no known competing financial interests or personal relationships that could have appeared to influence the work reported in this paper.

Data Availability

No data was used for the research described in the article.

Acknowledgments

This work was supported by the Research Fund of the Korea Institute of Materials Science (KIMS) (No. PNK8350).

References

[1] K.I. Tserpes, V. Karachalios, I. Giannopoulos, V. Prentzias, R. Ruzek, Strain and damage monitoring in CFRP fuselage panels using fiber Bragg grating sensors. Part I: design, manufacturing and impact testing, Compos. Struct. 107 (2014) 726–736, https://doi.org/10.1016/j.compstruct.2013.09.053.

[2] J.A. Artero-Guerrero, J. Pernas-Sánchez, J. López-Puente, D. Varas, On the influence of filling level in CFRP aircraft fuel tank subjected to high velocity impacts, Compos. Struct. 107 (2014) 570–577, https://doi.org/10.1016/j.compstruct.2013.08.036.

[3] M. Carello, A.G. Airale, A. Ferraris, A. Messana, L. Sisca, Static design and finite element analysis of innovative CFRP transverse leaf spring, Appl. Compos. Mater. 24 (2017) 1493–1508, https://doi.org/10.1007/s10443-017-9596-6.

[4] M. Corradi, C. Mouli Vemury, V. Edmondson, K. Pologanathan, B. Nagaratnam, Local FRP reinforcement of existing timber beams, Compos. Struct. 258 (2021), https://doi.org/10.1016/j.compstruct.2020.113363. ⟨http://www.ncbi.nlm.nih.gov/pubmed/113363⟩.

[5] Y. Liu, B. Zwingmann, M. Schlaich, Carbon fiber reinforced polymer for cable structures—a review, Polymers 7 (2015) 2078–2099, https://doi.org/10.3390/polym7101501.

[6] A. Hosoi, S. Sakuma, Y. Fujita, H. Kawada, Prediction of initiation of transverse cracks in cross-ply CFRP laminates under fatigue loading by fatigue properties of unidirectional CFRP in 90° direction, Compos. A 68 (2015) 398–405, https://doi.org/10.1016/j.compositesa.2014.10.022.

[7] E. Kappel, D. Stefaniak, C. Hühne, Process distortions in prepreg manufacturing – an experimental study on CFRP L-profiles, Compos. Struct. 106 (2013) 615–625, https://doi.org/10.1016/j.compstruct.2013.07.020.

[8] M. Perner, S. Algermissen, R. Keimer, H.P. Monner, Avoiding defects in manufacturing processes: a review for automated CFRP production, Robot.

Comput. Integr. Manuf. 38 (2016) 82–92, https://doi.org/10.1016/j.rcim.2015.10.008.
[9] E. Kappel, D. Stefaniak, D. Holzhüter, C. Hühne, M. Sinapius, Manufacturing distortions of a CFRP box-structure – a semi-numerical prediction approach, Compos. A 51 (2013) 89–98, https://doi.org/10.1016/j.compositesa.2013.04.003.
[10] S.J. Thompson, S. Bichon, R.J. Grant, Influence of ply misalignment on form error in the manufacturing of CFRP mirrors, Opt. Mater. Express 4 (2014) 79–91, https://doi.org/10.1364/OME.4.000079.
[11] A. Vita, V. Castorani, M. Germani, M. Marconi, Comparative life cycle assessment and cost analysis of autoclave and pressure bag molding for producing CFRP components, Int. J. Adv. Manuf. Technol. 105 (2019) 1967–1982, https://doi.org/10.1007/s00170-019-04384-9.
[12] V. McKenna, Y. Jin, A. Murphy, M. Morgan, R. Fu, X. Qin, et al., Cost-oriented process optimisation through variation propagation management for aircraft wing spar assembly, Robot. Comput. Integr. Manuf. 57 (2019) 435–451, https://doi.org/10.1016/j.rcim.2018.12.009.
[13] Z. Ge, X. Ding, Design of thermal error control system for high-speed motorized spindle based on thermal contraction of CFRP, Int. J. Mach. Tools Manuf. 125 (2018) 99–111, https://doi.org/10.1016/j.ijmachtools.2017.11.002.
[14] M. Torres, S. Piedra, S. Ledesma, A. Escalante-Velázquez, C, G. Angelucci, Manufacturing process of high performance-low cost composite structures for light sport aircrafts, Aerospace 6 (2019) 11.
[15] X. Liu, J. Li, J. Zhu, Y. Wang, X. Qing, Cure monitoring and damage identification of CFRP using embedded piezoelectric sensors network, Ultrasonics 115 (2021), 106470, https://doi.org/10.1016/j.ultras.2021.106470.
[16] M. Kahali Moghaddam, M. Hübner, M. Koerdt, C. Brauner, W. Lang, Sensors on a plasticized thermoset substrate for cure monitoring of CFRP production, Sens. Actuators A 267 (2017) 560–566, https://doi.org/10.1016/j.sna.2017.10.007.
[17] J. Huang, J. Zeng, Y. Bai, Y. Wang, K. Wang, X. Wu, et al., Real-time monitoring for the CFRP/aluminium-alloy bonding structure during curing process using encapsulated fiber Bragg grating sensor, Opt. Fiber Technol. 57 (2020), https://doi.org/10.1016/j.yofte.2020.102216. ⟨http://www.ncbi.nlm.nih.gov/pubmed/102216⟩.
[18] H. Kim, D. Kang, M. Kim, M.H. Jung, Microwave curing characteristics of CFRP composite depending on thickness variation using FBG temperature, Sens. Mater. 13 (2020) 1720.
[19] K.P. Ma, C.W. Wu, Y.T. Tsai, Y.C. Hsu, C.C. Chiang, Internal residual strain measurements in carbon fiber-reinforced polymer laminates curing process using embedded tilted fiber Bragg grating sensor, Polymers 12 (2020) 1479, https://doi.org/10.3390/polym12071479.
[20] C.B. Jiang, L.H. Zhan, X.B. Yang, X.P. Chen, Z.J. Lin, C.L. Guan, Monitoring of multidirectional and cure-induced strain in CFRP laminates using FBG sensors, Mater. Sci. Forum 953 (2019) 72–79, https://doi.org/10.4028/www.scientific.net/MSF.953.72.
[21] F. Zhou, J. Zhang, S. Song, D. Yang, C. Wang, Effect of temperature on material properties of carbon fiber reinforced polymer (CFRP) tendons: Experiments and model assessment, Materials 12 (2019) 1025, https://doi.org/10.3390/ma12071025.
[22] K. Mizukami, Evaluation of size of surface and subsurface waviness in carbon fiber composites using eddy current testing: a numerical study, Adv. Compos. Mater. 27 (2018) 589–604, https://doi.org/10.1080/09243046.2017.1417092.
[23] K. Mizukami, Y. Mizutani, A. Todoroki, Y. Suzuki, Analytical solutions to eddy current in carbon fiber-reinforced composites induced by line current, Adv. Compos. Mater. 25 (2016) 385–401, https://doi.org/10.1080/09243046.2015.1052132.
[24] K. Mizukami, K. Ogi, Non-contact visualization of fiber waviness distribution in carbon fiber composites using eddy current testing, Adv. Compos. Mater. 27 (2018) 135–146, https://doi.org/10.1080/09243046.2017.1344917.
[25] K. Mizukami, T. Ikeda, K. Ogi, Ultrasonic guided wave technique for monitoring cure-dependent viscoelastic properties of carbon fiber composites with toughened interlaminar layers, Adv. Compos. Mater. 30 (2) (2021) 85–105, https://doi.org/10.1080/09243046.2020.1812801.
[26] M.A. Ali, K.A. Khan, R. Umer, An electric circuit analogy-based homogenization approach for predicting the effective permeability of complex dual-scale porous media, Mater. Today Commun. 28 (2021), 102565, https://doi.org/10.1016/j.mtcomm.2021.102565.
[27] H. Rocha, C. Fernandes, N. Ferreira, U. Lafont, J.P. Nunes, Damage localization on CFRP composites by electrical impedance tomography, Mater. Today Commun. 32 (2022), 104164, https://doi.org/10.1016/j.mtcomm.2022.104164.
[28] C.M. Murray, S.M. Doshi, D.H. Sung, E.T. Thostenson, Hierarchical composites with electrophoretically deposited carbon nanotubes for in situ sensing of deformation and damage, Nanomaterials 10 (2020) 1262, https://doi.org/10.3390/nano10071262.
[29] S.M. Doshi, C.M. Murray, A. Chaudhari, D.H. Sung, E.T. Thostenson, Ultrahigh sensitivity wearable sensors enabled by electrophoretic deposition of carbon nanostructured composites onto everyday fabrics, J. Mater. Chem. C 10 (2022) 1617–1624, https://doi.org/10.1039/d1tc05132f.
[30] D.H. Sung, S.M. Doshi, C.M. Murray, A.N. Rider, E.T. Thostenson, Electrophoretic deposition: Novel in situ film growth mechanism of carbon nanocomposite films within non-conductive fabrics for multi-scale hybrid composites, Compos. Sci. Technol. 200 (2020), 108415, https://doi.org/10.1016/j.compscitech.2020.108415.
[31] Y.-H. Zhou, C.-Y. Chen, B.-L. Li, K.-Q. Chen, Characteristics of classical Kirchhoff's superposition law in carbon atomic wires connected in parallel, Carbon 95 (2015) 503–510, https://doi.org/10.1016/j.carbon.2015.08.064.
[32] P. Zhu, E. Crus-Silva, V. Meunier, Electronic transport properties in graphene oxide frameworks, Phys. Rev. B 89 (2014), 085427, https://doi.org/10.1103/PhysRevB.89.085427.
[33] J.B. Park, T. Okabe, N. Takeda, W.A. Curtin, Electromechanical modeling of unidirectional CFRP composites under tensile loading condition, Compos. A 33 (2002) 267–275, https://doi.org/10.1016/S1359-835X(01)00097-5.
[34] Z. Xia, T. Okabe, J.B. Park, W.A. Curtin, N. Takeda, Quantitative damage detection in CFRP composites: coupled mechanical and electrical models, Compos. Sci. Technol. 63 (2003) 1411–1422, https://doi.org/10.1016/S0266-3538(03)00083-6.